Influence of the change in physical properties of sewage sludge during biochar production on its fluid dynamic behavior

Biomass Conversion and Biorefinery (2026) 16:212
https://doi.org/10.1007/s13399-026-07118-6

ORIGINAL ARTICLE

Influence of the change in physical properties of sewage sludge during biochar production on its fluid dynamic behavior

Andrés Felipe Pardo Martínez[1] · David Felipe Torres Arce[1] · Jorge Esteban Valbuena Mejía[1] · Diana Carolina Guío-Pérez[2] · Sonia Lucía Rincón Prat[1]

Received: 16 May 2025 / Revised: 18 January 2026 / Accepted: 7 March 2026 / Published online: 23 April 2026

Abstract

Despite the relevance of physical properties on the fluid dynamic behavior of binary beds, the physical transformation of feedstock particles during pyrolysis is often overlooked. The present work aims at studying the variation of physical properties of sewage sludge during biochar production and assessing the impact of such change on the fluid-dynamic behavior of binary mixtures with silica sand. Sewage sludge was obtained from the municipal wastewater treatment plant of the city of Bogotá, D.C. Biochar samples were produced through pyrolysis in a thin layer fixed bed reactor at 450 °C, 550 °C and 650 °C under heating rates of about 5 K/s. Three different particle sizes of the initial sewage sludge samples were studied (106 µm to 150 µm, 150 µm to 212 µm, and 300 µm to 500 µm). Particle size and particle density of the original sewage sludge and the produced biochar samples were measured. It was found that the reduction in particle mean diameter at the highest temperature was of 19% and for the particle density the reduction was of 29%. The fluidization behavior of the biochar samples mixed with silica sand (approximately 20% char to 80% sand in volume) was studied in a cold flow model and the minimum fluidization velocity of the mixtures (u_{mf}) was experimentally determined. The ability of different correlations reported in the literature to accurately predict the minimum fluidization velocity of the obtained biochars – sand mixtures was evaluated. Even though some qualitative changes in the fluid dynamic behavior of the mixtures were identified as a result of the change in properties, no clear quantitative change in the minimum fluidization velocity could be observed. On the one hand, the reduction in particle mean diameter and in particle density does not present relevant changes in the Geldart classification of the fuel particle, and on the other hand, the fuel particles are prone to segregate creating an overlap in the minimum fluidization velocity of the two different solid phases.

Keywords Sewage sludge · Pyrolysis · Fluidized bed · Biochar · Fluid-dynamic analysis

Nomenclature

Ar	Arquimedes number of the particle
D	Diameter of the reactor m
d_{p}	Particle diameter mm
$d_{\mathrm{p,eff}}$	Effective particle diameter mm
d^*	Dimensionless particle diameter
h_{mf}	High of the bed at minimum fluidization conditions m
m	Mass kg
Re	Reynolds number of the particle
u	Gas velocity $^{cm}/_{s}$
u	Gas velocity $^{cm}/_{s}$
u_{mf}	Minimum fluidization velocity $^{cm}/_{s}$
u^*	Dimensionless velocity
x	Weight fraction $\%$
$\triangle p$	Pressure drop Pa
ϵ_{mf}	Voidage at minimum fluidizing conditions $\%$
μ	Gas viscosity Pas
ρ_b	Bulk density $^{kg}/_{m^3}$

✉ Andrés Felipe Pardo Martínez
afpardom@unal.edu.co

[1] Faculty of Engineering, Department of Mechanical and Mechatronics Engineering, Research Group on Biomass and Optimization of Thermal Processes-BIOT, National University of Colombia-Bogotá, Carrera 30 No 45A-03 Building 453, Bogotá, Colombia

[2] Division of Energy Technology, Chalmers University of Technology, Hörsalsvägen 7B, Göteborg 412 96, Sweden

ρ_{eff}	Effective particle density $^{kg}/_{m^3}$
ρ_{g}	Gas density $^{kg}/_{m^3}$
ρ_{s}	Particle density $^{kg}/_{m^3}$
φ_s	sphericity %
WWTP	Waste water treatment plant
SS	Sewage sludge

1 Introduction

Global population grows at an annual rate of approximately 1.05% [1], combined with ongoing industrialization, has led to a significant increase in the generation of waste and industrial residues, including solid, liquid, and gaseous forms. To mitigate water pollution, globally wastewater treatment plants (WWTPs) have been established in major cities. These plants clean the water and concentrate pollutants into an organic byproduct called Sewage sludge [2, 3]. In the city of Bogotá, Colombia alone, nearly 300 tons of sewage sludge are generated every day [4], the problem with this sewage sludge is that they require large and special facilities for their disposal.

The final disposal of sewage sludge is currently carried out through three main pathways: landfilling, agricultural use, and incineration [5]. In several European countries more than 80% of the generated sewage sludge is disposed of through incineration [6] a highly mature and established process. Incineration, along with other thermochemical treatments such as pyrolysis, drying, and gasification, is employed to reduce both the environmental impact and the volume of sewage sludge. Pyrolysis, a widely adopted alternative, involves the thermal decomposition of organic material in an inert atmosphere, producing gases, liquids, and a solid carbon-rich residue known as biochar [7]. Due to the high ash content of sewage sludge, the biochar yield can be relatively high—approximately 50%. Among the various technologies available for sludge pyrolysis, fluidized bed reactors are often preferred in both industrial and research settings due to their lower cost, ease of operation, and scalability compared to other reactor types [8, 9]. It is important to note that its properties and composition can vary significantly depending on its origin. This variability necessitates thorough characterization of its physical, compositional, and fluid-dynamic properties to ensure its suitability for applications such as fluidized bed systems.

Multiple researchers have analyzed the fluidization behavior of binary mixtures in fluidized bed reactors to develop correlations that enable the prediction of fluidization behavior based on the physical properties of the particles involved [10]. Properties such as particle density, skeletal density, bulk density, void fraction, mean equivalent diameter, and particle shape significantly influence the minimum fluidization velocity (u_{mf}) a key parameter for the operation of this type of reactor fluidization behavior is particularly affected by particle size and density [10]. Zhong et al. [11] observed that, in beds composed of various biomasses and sand, an increase in effective particle density results in a corresponding increase in u_{mf}. Similarly Rao et al. [12] reported a direct correlation between particle size and density and the minimum fluidization velocity. Beyond fluidization velocity, other aspects of fluidization behavior are also influenced by particle characteristics. Clarke et al. [13] found that large differences in particle size and density between the biomass and the bed material lead to significant segregation within the mixture. Berruti et al. [14] further reported that, for low-density biomass, particle entrainment, mixing, and segregation are strongly affected by particle size and density.

Several authors have studied the fluidization of binary mixtures of biomass and sand [11–13, 15–17]. However, few studies have focused on the fluidization behavior after the pyrolysis process—an important consideration in systems with continuous feed, where fluidization persists beyond the thermochemical conversion stage. Since pyrolysis alters key particle properties relevant to fluidization [18], it is essential to understand both the nature and extent of these changes in order to maintain stable and uniform fluidization throughout the process. Moreover, determining whether operational adjustments are necessary depends on accurately characterizing these transformations. Given that pyrolysis-induced changes in particle properties can directly affect fluidization dynamics, the performance and regime of the fluidized bed may not be reliably predicted without accounting for such variations. Therefore, it is crucial to quantify the magnitude of these property changes and assess their potential impact on the fluidization behavior of the resulting biochar–sand mixtures.

This study aims to enhance the understanding of the fluidization behavior of sewage sludge and its derived biochars during the pyrolysis process. It will examine the influence of the initial particle size of sewage sludge and the change in its physical properties during processing on fluidization characteristics. To replicate the heating rates typically observed in fluidized bed reactors, fast pyrolysis of sewage sludge was performed in a thin layer fixed bed reactor under high heating rates (approximately 5–6 °C/s). The pyrolysis experiments were conducted at three different temperatures (450 °C, 550 °C, and 650 °C) in a nitrogen atmosphere, using a fixed mass of sewage sludge and three different mean particle size ranges. Following pyrolysis, the resulting biochar (solid product) was analyzed to evaluate changes in particle density and mean particle diameter. Based on the

properties of both the raw sewage sludge and the produced biochar, changes in the Geldart classification of the particles [19] were also investigated.

Additionally, a fluid dynamic analysis of mixtures of sewage sludge or biochar mixed with sand (as bed material) was performed in a cold flow model of a fluidized bed reactor. Minimum fluidization velocity (u_{mf}) was obtained from fluidization curves, and a visual analysis of the fluidization behavior was performed. Experimental values of u_{mf} were compared with values obtained using empirical correlations from literature and the implementation of effective physical properties of the mixtures and the most appropriate ones were determined. Finally, an analysis of the effect of temperature and fluidization velocity during biochar production on the fluidization regime and the Geldart classification of the particles was studied using the Grace diagram [20]. Based on the findings, it will be possible to determine whether adjustments in fluidization velocity are necessary during the conversion from sewage sludge to biochar.

2 Materials and methods

2.1 Sewage sludge and bed material properties

Sewage sludge (SS) was obtained from the El Salitre wastewater treatment plant in Bogotá, D.C. (Colombia). Following collection, the sludge was dried for 30 days in a greenhouse, where daytime temperatures were maintained at approximately 45 °C. Subsequently, the sample was oven-dried at 81 °C for 24 h until a final moisture content of approximately 6% was achieved. On a dry basis, the ash content and volatile matter were found to be 40.4% and 51.2%, respectively. After drying, the sewage sludge was crushed to a particle size of approximately 4 mm—first manually (hammering) and then using a Retsch SM100 mill. The material was then further ground using the same mill and a manual grinder and sieved to obtain three particle size fractions for testing, using a Vibratory Sieve Shaker (ANALYSETTE 3 PRO): 500 µm to 300 µm, 212 µm to 150 µm, and finally from 150 µm to 106 µm. Each particle size fraction is obtained from a separate batch of the initial 4 mm sample. The sample is milled and ground until the desired particle size is reached. This is repeated until the required mass for further analysis is obtained.

Particle density was measured using the powder pycnometry method described by Buczek and Geldart [21]. This method was implemented as an alternative to the traditional pycnometer technique using a liquid medium, due to the rapid absorption of the liquid by sewage sludge and biochar particles. When the particles were introduced into the liquid, they initially floated but submerged within less than a minute. This behavior indicates a change in particle density over time, leading to inaccuracies in the measurement process. The method involves measuring the bulk density of a bed of fine particles, followed by tapping the container several times (200 times for this study) to allow the particles to settle and fill the void spaces between them. The bulk density is then measured again to obtain the tapped bulk density. This procedure is subsequently repeated with the addition of the feedstock particles whose density is to be determined. Finally, the tapped bulk density of the mixture of sand and feedstock is compared to the tapped bulk density of the sand alone, and the difference is used to estimate the particle density of the feedstock. As pycnometric powder sand with a mean diameter of 90 µm was used (this sand classified in Geldart A group which is helpful because does not have cohesive properties), the volume of the used recipient was 32 ml, 1.5 g of feedstock and between 43 and 44 g of sand were used.

2.2 Experimental facility and procedure

Two experimental setups were used in this study: a biochar production facility and a cold-flow model of a fluidized bed reactor. The biochar production facility is shown in Fig. 1. It enables biochar generation under high heating rates (up to 5 K/s) and allows for rapid quenching of the sample after processing. It consists of three main components: a heating section, a cooling section, and a movable sample holder. The sample holder features a crank mechanism that drives a worm screw, enabling the transfer of the sample container between the cooling and heating sections. The sample container is a rectangular basket (18 cm × 13 cm × 3 cm) made of stainless-steel mesh No. 140 (105 µm). For each run, 80 g of raw sewage sludge with a selected particle size fraction were loaded into the sample holder (approximately 1 cm bed height) and initially placed in the left side of the cooling section. After assembly, the reactor in the heating section was preheated to 750 °C over a period of 5 h. During this time, the temperature of the sludge sample in the cooling section was continuously monitored to prevent premature reactions. According to Mendoza et al. [8] mass loss in sewage sludge pyrolysis remains below 2% of the initial mass at temperatures up to 200 °C. In the present experiments, the maximum temperature recorded in the cooling section was 170 °C, implying that mass loss during this stage was likely below 1%. A continuous nitrogen flow of 0.5 L/min was introduced at the rear of the cooling section to maintain an inert atmosphere. Once the reactor reached 750 °C, the sample was rapidly transferred into the heating section using the crank-driven mechanism. The sample was exposed to the target pyrolysis temperature (450 °C, 550 °C, or 650 °C), and upon reaching this temperature, it was immediately returned to the cooling section. The temperature

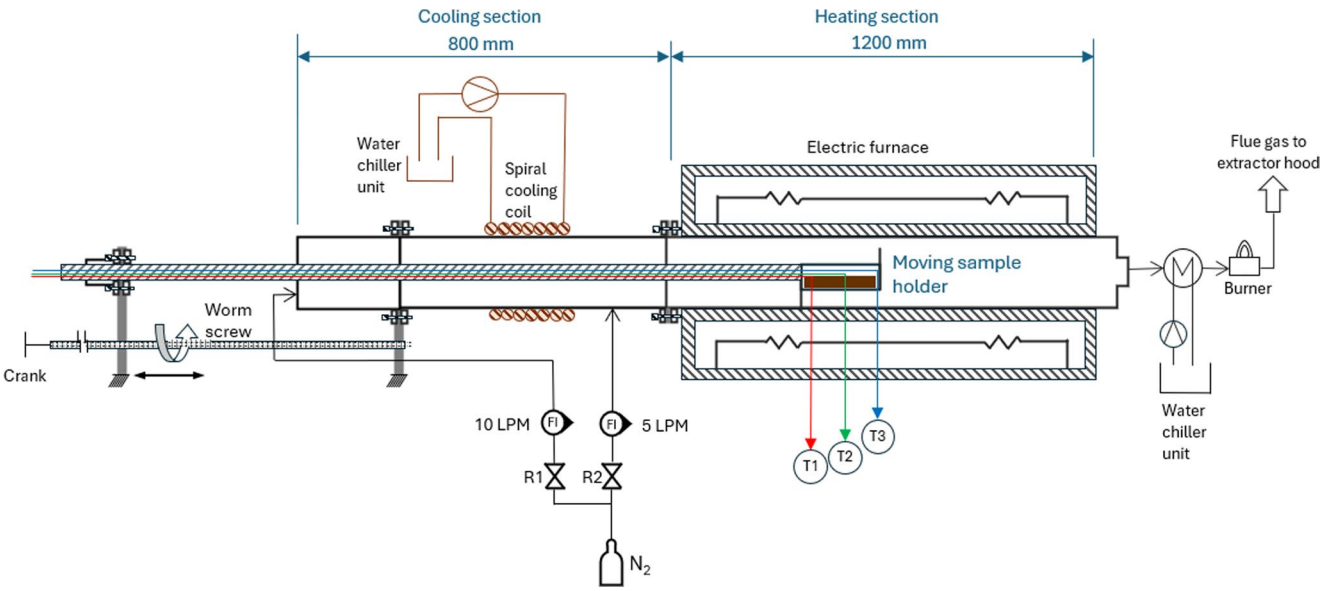

Fig. 1 Schematic diagram of the facility for biochar production

in the cooling zone dropped to 170 °C within 5 min, effectively halting any further thermal reactions in the biochar. A downstream heat exchanger and burner were used to treat the gases produced during pyrolysis. After cooling, the biochar sample obtained is removed from the reactor and weighed. The biochar yield is determined as the relationship between the final mass of biochar and the initial mass of sewage sludge introduced in the reactor bed.

The cold-flow model and its schematic diagram are presented in Fig. 2. The setup consists of a cylindrical

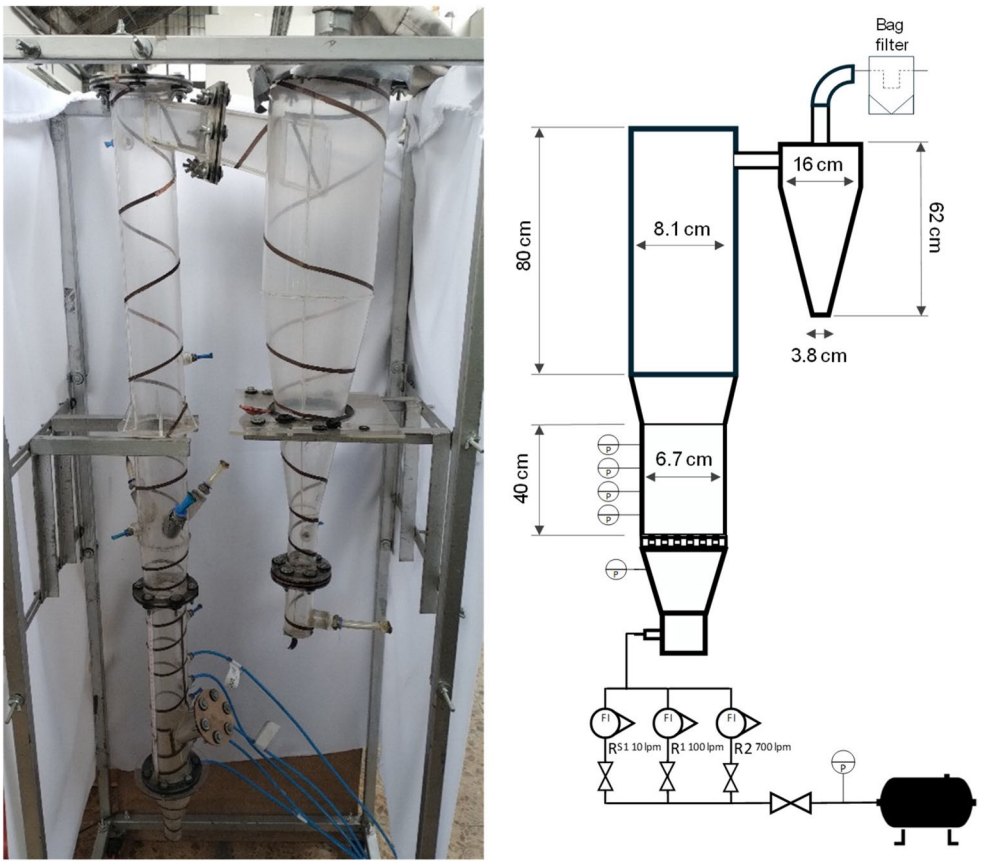

Fig. 2 Cold flow model of a fluidized bed reactor

fluidization chamber divided into two zones: the lower zone has an inner diameter of 6.7 cm and a length of 40 cm, while the upper zone has an inner diameter of 8.1 cm and a length of 80 cm. The lower zone includes a gas distributor composed of a flat perforated plate with 1 mm diameter circular holes arranged in a triangular pattern. This plate is covered with a fabric that permits air flow while preventing bed particles from falling through. Additionally, five pressure measurement ports are located in the lower zone: one below the distributor and four above it. The fluidization chamber is connected to a cyclone separator, which is 62 cm in length and has inner diameters of 16 cm and 3.8 cm. A filter bag is installed at the top of the cyclone to allow the exit of air while capturing fine particles. Airflow is regulated using three rotameters with maximum flow capacities of 10 L/min, 100 L/min, and 700 L/min, respectively. The cold-flow model was employed to generate fluidization curves for each mixture of sewage sludge or biochar with sand. From these curves, the minimum fluidization velocity (u_{mf}) for each mixture was determined.

2.3 Experimental plan

Variations in physical properties during biochar production are caused by the reaction progress which in turn depends on the final pyrolysis temperature. To obtain biochar samples at different stages of the pyrolysis reaction experiments with final pyrolysis temperatures of 450 °C, 550 °C, and 650 °C for each of the particle size ranges described in Sect. 2.1. were performed. A total of a total of 9 biochar samples were obtained. These temperatures were selected because they are representative of typical operating conditions in pyrolysis processes [8]. The experiments are identified using the following nomenclature: B-Temperature-Particle Size (where 106 µm – 150 µm=S, 150 µm – 212 µm=M, and 300 µm – 500 µm=L). For example, the experiment labeled B450-S refers to biochar production at 450 °C using the particle size range of 106 µm–150 µm.

Fluidization curves were generated for each particle size range of both the raw sewage sludge and the resulting biochar samples for a total of 12 experiments. All experiments were conducted using sand as the bed material with a fixed volume ratio of 80% sand − 20% sewage sludge or biochar. This ratio was chosen based on preliminary testing, which demonstrated good fluidization performance for 80% – 20% mixtures, as well as for 85% – 15% and 90% – 10% ratios. The 80% – 20% ratio was selected to maximize the amount of feedstock used in the experiments.

The fluidization experiments are denoted by adding an "F" prefix to the biochar experiment codes described above (e.g., F-B450-S). For raw sewage sludge samples, the notation F-SS-S, F-SS-M, or F-SS-L was used, depending on particle size.

2.4 Data analysis and calculations

2.4.1 Experimental determination of the minimum fluidization velocity (u_{mf}) of the binary mixtures

The value of u_{mf} is determined by measuring the fluidization curve of mixtures of sewage sludge or biochar and bed material (sand) following the procedure established by Kunii and Levenspiel [10]. A fluidization curve shows the pressure drop of a gas flow passing through a bed of particles as the gas velocity increases. At low gas velocities, the system behaves as a fixed bed, and the pressure drop across the bed increases linearly with the gas velocity until a maximum value (Δp_{max}) is reached. As the gas velocity increases slightly beyond this point, the pressure drop decreases to a lower value corresponding to the onset of fluidization (Δp_{mf}). This reduction in pressure drop is primarily observed in beds with uniform particle sizes and is attributed to effects such as bed pre-compaction and wall effects [10]. As the gas velocity continues to increase, the pressure differential across the bed remains nearly constant, indicating that the bed has reached the fluidized state. At this stage, the mixture of gas and solid particles behaves like a fluid, deforming easily and offering minimal resistance to flow [10]. Consequently, the fluidization curve exhibits a segment with an approximately zero slope. As a reference Fig. 6 shows experimental curves obtained in this work. To determine the value of u_{mf}, two trend lines are projected: one corresponding to the linear increase in pressure drop prior to fluidization, and another representing the region where the pressure drop stabilizes. The intersection of these two lines defines the value of u_{mf}. Finally, when the pneumatic transport velocity (u_t) is reached, the pressure drop may either increase, due to enhanced frictional forces, or decrease, as a result of the reduced number of particles remaining within the reactor [22].

2.4.2 Theorical determination of the minimum fluidization velocity (u_{mf}) of the binary mixtures

Numerous models have been developed to estimate the minimum fluidization velocity, most of them derived from the Ergun Eqs. [10, 23]. This equation relates the inertial forces acting on a particle to the drag force exerted by a fluid flowing over it. To apply the Ergun equation, it is necessary to determine the Archimedes number (Ar), the Reynolds number (Re), the bed voidage at minimum fluidization conditions (ϵ_{mf}) and the particle sphericity (φ_s). For irregularly shaped particles or inhomogeneous beds, accurately measuring voidage and sphericity can be particularly challenging. In cases where these parameters are unknown or cannot

be reliably estimated, the simplified form of the Ergun equation shown in Eq. 1 is used.

$$C_1 \mathrm{Re}_{\mathrm{mf}}^2 + C_2 \mathrm{Re}_{\mathrm{mf}} - \mathrm{Ar} = 0 \tag{1}$$

$\mathrm{Re}_{\mathrm{mf}}$ and Ar are calculated from their definitions:

$$\mathrm{Re}_{\mathrm{mf}} = \frac{d_{\mathrm{p}} u_{\mathrm{mf}} \rho_{\mathrm{g}}}{\mu} \tag{2}$$

$$\mathrm{Ar} = \frac{{d_{\mathrm{p}}}^3 \rho_{\mathrm{g}} (\rho_{\mathrm{s}} - \rho_{\mathrm{g}}) g}{\mu^2} \tag{3}$$

The values of C_1 and C_2 relate the voidage of the bed and the sphericity, these can be theoretically determined using the expressions presented in Table 1 for the Ergun equation or based on empirical correlation factors determined from experimental studies. Different research works have been carried out to establish the values of C_1 and C_2 that allow an accurate determination of the minimum fluidization velocity for different types of particles. In their literature review, Gupta et al. [30] compiled over 60 values proposed by different authors, highlighting the complexity of theoretically predicting the fluidization behavior of a particle bed. This challenge becomes even greater when the bed consists of two or more types of particles. With the values of C_1 and C_2 Eq. 1 can be solved to find the value of $\mathrm{Re}_{\mathrm{mf}}$ and then the value of u_{mf} can be obtained. Table 1 presents a compilation of the most frequently used empirical correlation factors found in literature [10, 22].

Table 1 Empirical correlation factors C_1 and C_2 to be used in Eq. 1 according to different authors

Author	C_1	C_2
Ergun [10]	$\frac{1.75}{\epsilon_{\mathrm{mf}}^3 \phi_{\mathrm{s}}}$	$\frac{150(1-\epsilon_{\mathrm{mf}})}{\epsilon_{\mathrm{mf}}^3 \phi_s^2}$
Wen and Yu [24]	24.5	1652.0
Richardson et al. [25]	27.4	1408.2
Saxena and Vogel [26]	17.5	886.2
Babu et al. [27]	15.4	777.3
Grace [28]	24.5	1333.3
Chitester et al. [29]	20.2	1161.9

To use Eq. 1 for a bed of a binary mixture effective values for the mean particle diameter ($d_{\mathrm{p,eff}}$) and particle density ($\rho_{\mathrm{s,eff}}$) must be calculated. These effective properties also allow for the calculation of the corresponding effective $\mathrm{Re}_{\mathrm{mf,\ eff}}$ and $\mathrm{Ar}_{\mathrm{eff}}$ numbers to be used in Eq. 1. Following the methodology proposed by Chongdian et al. [31] and Cáceres-Martínez et al. [22] the effective particle diameter and particle density are calculated using Eq. 4 and Eq. 5 respectively, with 1 meaning the properties of sewage sludge and 2 the properties of the sand used as bed material.

$$d_{\mathrm{p,eff}} = d_{\mathrm{p1}} d_{\mathrm{p2}} \left(\frac{x_1 \rho_{\mathrm{s2}} + x_2 \rho_{\mathrm{s1}}}{x_1 \rho_{\mathrm{s2}} \mathrm{d}_{\mathrm{p2}} + x_2 \rho_{\mathrm{s1}} \mathrm{d}_{\mathrm{p2}}} \right) \tag{4}$$

$$\frac{1}{\rho_{\mathrm{s,eff}}} = \frac{x_1}{\rho_{\mathrm{s1}}} + \frac{x_2}{\rho_{\mathrm{s2}}} \tag{5}$$

The determination of the theoretical values of C_1 and C_2 derived from the Ergun equation requires the knowledge of the the voidage (ϵ_{mf}) and the sphericity (ϕ_{s}) as shown in Table 1. Voidage was determined using Eq. 4 where h_{mf} is the height of the bed at minimum fluidization conditions, D is the diameter of the reactor, m is the mass of the sand or the feedstock and ρ_{s} is the particle density. Equation 4 establish that the relation between the difference of the actual bed volume at minimum fluidizing conditions and the volume of the bed assuming that there is no space between particles to the to the actual bed volume at minimum fluidizing conditions represents the voidage of the bed.

$$\epsilon_{\mathrm{mf}} = \frac{V_{\mathrm{total}} - (V_{\mathrm{sand}} + V_{\mathrm{feedstock}})}{V_{\mathrm{total}}} = 1 - \frac{\frac{m_{\mathrm{sand}}}{\rho_{\mathrm{s,sand}}} + \frac{m_{\mathrm{feedstock}}}{\rho_{\mathrm{s,feedstock}}}}{\left(\pi \frac{D^2}{4}\right) h_{\mathrm{mf}}} \tag{6}$$

Sphericity was estimated as the relationship between the mean volume of the particles by assuming an ellipsoidal shape (with dimensions *l*, length; *p*, depth and *h*, height) and the volume of a sphere with a diameter equal to the average value of the three previous dimensions, as shown in Eq. 7. Measurements of *l*, *p* and *h* were made on 15 sewage sludge and biochar particles using an Alicona Infinite Focus G5 focus variation microscope. Figure 3

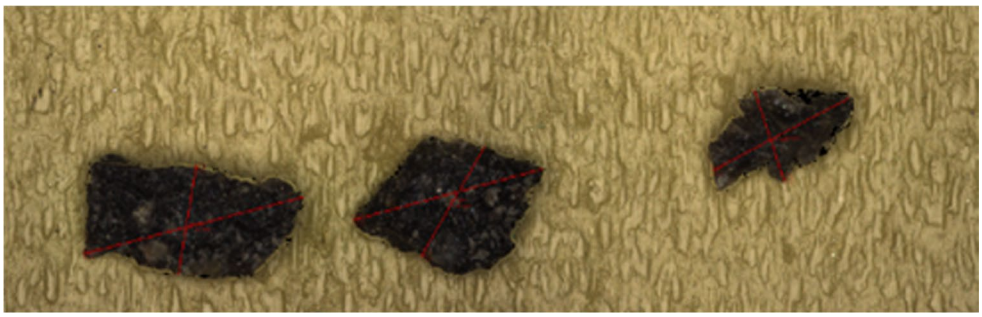

Fig. 3 Picture of three char particles and the lines representing the measure of length and width

shows an example of the images and the measurements made for three particles.

$$\phi = \frac{V_{ellipsoid}}{V_{sphere}} = \frac{{}^{4}/_{3}\,\pi lph}{{}^{4}/_{3}\,\pi\left[\frac{l+p+h}{3}\right]^{3}} \tag{7}$$

2.4.3 Mapping of fluidization regimes

Once the minimum fluidization velocity has been established the Grace diagram [10] is used to analyze the fluidization regimes during biochar production from the sewage sludge samples studied in this work. The Grace diagram identifies areas for the different fluidization regimes according to the relationship between the dimensionless particle diameter and velocity calculated according to Eqs. 8 and9.

$$u^{*} = u\left[\frac{\rho_{g}^{2}}{\mu_{g}\left(\rho_{s}-\rho_{g}\right)g}\right]^{1/3} \tag{8}$$

$$d^{*} = d_{p}\left[\frac{\rho_{g}\left(\rho_{s}-\rho_{g}\right)g}{\mu_{g}^{2}}\right]^{1/3} \tag{9}$$

The analysis in this work includes the determination of the fluidization regime when the minimum fluidization velocity is implemented at ambient temperature and by processing temperature. Additionally, the influence of an increment in the fluidization velocity up to 3 u_{mf} (which is a value typically used in fluidized bed reactors) in the fluidization regime is determined.

3 Results and discussion

3.1 Particle properties

Figure 4 shows the results of particle mean diameter (Fig. 4 (a)) and particle density (Fig. 4 (b)) vs. biochar yield for each biochar sample obtained in this work. Tables 1 and 2 of supplementary material present the numerical values obtained. The first point from right to left of each figure represents the initial values of sewage sludge (yield of 100%) while the second to fourth points of each property correspond to the samples obtained at final pyrolysis temperatures of 450 °C, 550 °C and 650 °C respectively. As expected, an increase in pyrolysis temperature decreases the biochar yield. Moreover, a linear relationship between both particle size and density with biochar yield is obtained.

Regarding particle size, it can be observed that the slopes for the smaller size ranges are similar, while the largest

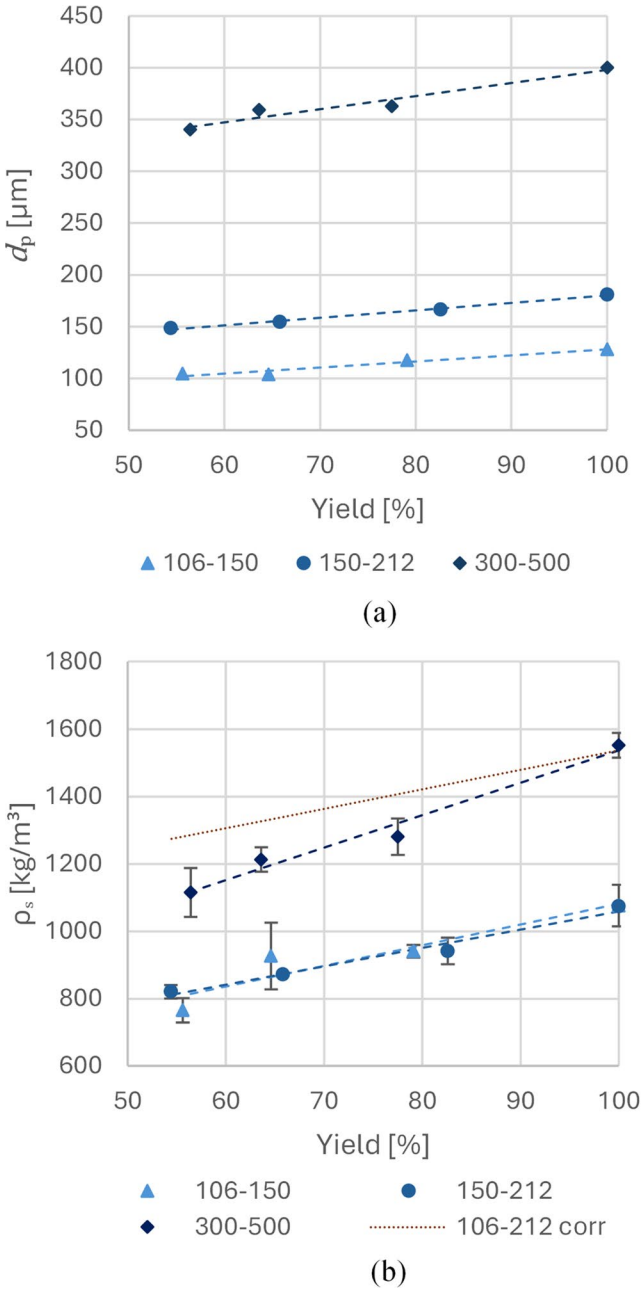

Fig. 4 Experimental values (marker) and tendency lines of particle properties vs. biochar yield. (**a**) Particle diameter. (**b**) Particle density

particle size exhibits a slightly greater reduction in mean diameter. This behavior may be attributed to the fact that, in larger particles, the pyrolysis reaction does not occur uniformly throughout the entire particle. Instead, due to internal heat transfer limitations, the reaction predominantly progresses from the outer surface toward the core. In contrast, smaller particles experience a more homogeneous mass loss throughout their volume.

For particle density, a similar trend is observed: the smaller particle sizes exhibit nearly identical slopes, while

the largest size displays a steeper slope. As previously mentioned, larger particles tend to experience less uniform heat transfer and more heterogeneous mass loss during pyrolysis. This non-uniform degradation may result in localized mass loss within the particle structure, leading to an increase in overall porosity and, consequently, a more pronounced decrease in particle density. The powder pycnometry method employed requires the reference powder (in this case, sand with a mean particle diameter of 90 µm) to be significantly smaller than the sample particles to ensure accurate measurements. Plantard et al. [32] observed by their measurements of particle density of activated carbons that for particle sizes with a size ratio (mean particle diameter of the pycnometric powder/mean particle diameter of the sample to be measured) higher than around 0.1 a reduction in particle density is obtained. The reduction increases with an increase in the size ratio being around 10% for a size ratio of 0.2 and almost 30% fr a size ratio of 0.5. For higher size ratios the decrease in density remains approximately constant at 30%. In this work for the small and medium sewage sludge and biochar particles the size ratio lies between 0.5 and 0.9, which may compromise the accuracy of the measurements and lead to an underestimation of the particle density. For the large particles the size ratio is much smaller, between 0.23 and 0.26, so these results are associated with less uncertainty in the measurement. To use a more accurate value of particle density in the subsequent analysis it is assumed that the physical properties of the sewage sludge samples are independent of the particle diameter (i.e., the grinding process does not affect the particle structure). Therefore, the particle density of sewage sludge is the same for all particles sizes used in this work and corresponds to the one obtained for particles between 300 and 500 µm. For the biochars of sewage sludge of small (106 µm – 150 µm) and medium (150 µm – 212 µm) particle sizes the reduction in particle density follows the same tendency as the one observed in Fig. 4 (b) giving the variation in particle density presented in the dotted line of the same figure.

3.2 Geldart classification

The results obtained in Sect. 3.1 were used to locate the particles in the Geldart chart [10]. Particles are classified in four groups according to their mean particle diameter and density in particles type A (aeratable), B (sand-like), C (cohesive) and D (spoutable). Particles in groups A (fluidize easily, showing smooth behavior at low gas velocities and small, controlled bubbles at higher velocities) and B (fluidize well, exhibiting vigorous bubbling and large bubble formation) are appropriate for fluidization purposes [10] while particles in groups C (cohesive or very fine powders that resist fluidization due to strong interparticle forces exceeding the fluidizing gas forces) and D (these are large and/or dense particles that are difficult to fluidize in deep beds, often showing erratic behavior such as large bubbles, channeling, or spouting under uneven gas distribution) are difficult to fluidize [10]. Figure 5 shows the location of the sewage particles and their biochars for each particle size range studied. The sand particles used in this work are also indicated. Particles of sewage sludge and chars in the ranges 106 µm to 150 µm fall into group A and particles in the range of 150 µm to 212 µm are located within the border of groups A and B. In the case of the sewage sludge and chars in the particle size range 300 µm to 500 µm the particles are in group B. The reduction in particle size and density with the advance of the pyrolysis reaction causes a displacement of the biochar particles in the Geldart diagram in direction left and down following a linear relationship. This reduction

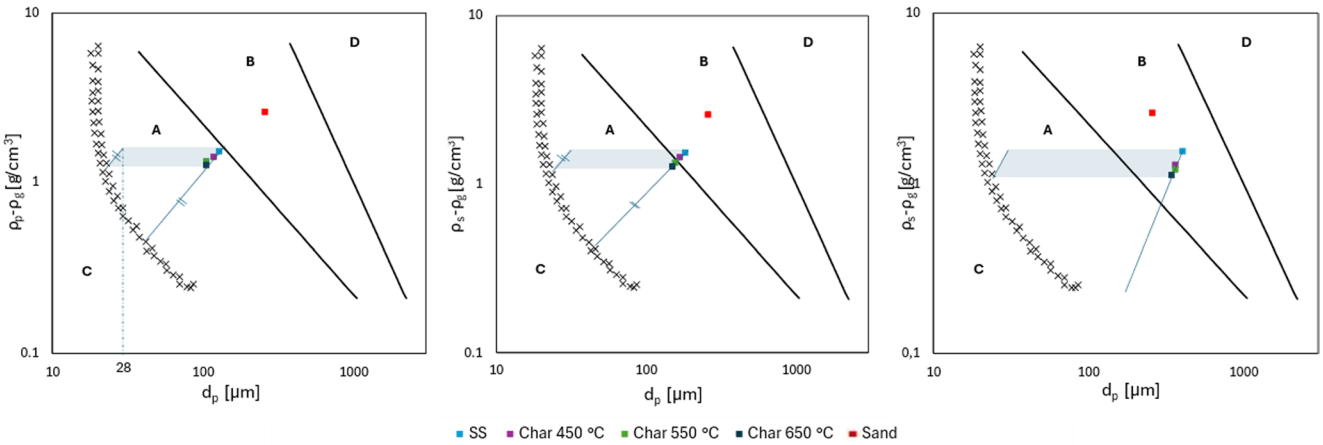

(a) FB 106-150 **(b)** FB 150-212 **(c)** FB 300-500

Fig. 5 Geldart classification chart for sewage sludge of the three mean particle diameters studied and its biochars. (**a**) FB 106–150, (**b**) FB 150–212, (**c**) FB 300–500

is, however, in all cases not big enough to move them to group C. Assuming that the particles will not have a reduction in particle density greater than the observed in these results despite of the initial size of the sewage sludge, the size of the sewage sludge can be reduce to almost 28 µm and the pyrolysis reaction will not turn the biochar particles into group C particles.

3.3 Minimum experimental fluidization velocity of sewage sludge – sand and sewage sludge biochar – sand mixtures

The fluidization curves obtained for sewage sludge – sand and sewage sludge biochar – sand mixtures were all very similar. All curves showed a clear zone for the fixed bed and for the fluidized bed zones. Figure 6 shows the fluidization curves for sewage sludge of particle diameter between 300 µm – 500 µm (Fig. 6 left) and its corresponding biochar generated at 450 °C (Fig. 6 right).

In both graphs of Fig. 6 two different slopes can be identified before reaching minimum fluidization velocity. This phenomenon happened in some of the experiments carried out and it is probably caused by the fact that the bed material (sand) and the feed stock (sewage sludge or char) reach fluidization at different velocities. The first zone with lower slope represents the behavior for the mix of sand and feedstock and the second zone with a higher slope represents the behavior of just the sand assuming that the feed stock has already reached the fluidization velocity, and it is no longer affecting the pressure drop. In the experiments where no difference in the slope is observed it is assumed that the behavior of the mix is almost the same as just the sand because the pressure drop caused by the feedstock is too low compared to the pressure drop caused by the sand.

Table 3 of supplementary material contains the results for minimum experimental fluidization velocity (u_{mf}) for all the mixtures used in this study. Figure 7 (a) show the results for minimum fluidization velocity (u_{mf}) compared to the particle mean diameter of sewage sludge and biochar and Fig. 7 (c) compared to the effective diameter of the mixture. The results show that increasing the mean particle diameter of the feedstock slightly increases the value of u_{mf} and the results are close to the ones obtained for the sand. Figure 7 (b) shows the results for minimum fluidization velocity (u_{mf}) compared to the particle density of sewage sludge and biochar and Fig. 7 (d) compared to the effective density of the mixture. The results show that an increase in the particle density of the feedstock also represents and slightly increase in the value of u_{mf} and the results are close to the ones obtained for the sand.

The Ergun equation is based on the principle that the drag force exerted by the upward-moving gas is equal to the weight of the particles. Since the mean particle diameter influences both the drag force and the weight, while the particle density affects only the weight, increases in either parameter are expected to raise the minimum fluidization velocity (u_{mf}). However, in this case, the fraction of sewage sludge is only 20%, and the proportion of biochar is even lower. As a result, the change in the effective particle diameter of the mixture is minimal. The variation in effective particle density is even smaller, given that the feedstock's particle density is nearly half that of sand. Consequently, changes in the mean particle diameter and density of the feedstock have little effect on the effective values, and therefore, the impact on the u_{mf} of the mixture is negligible.

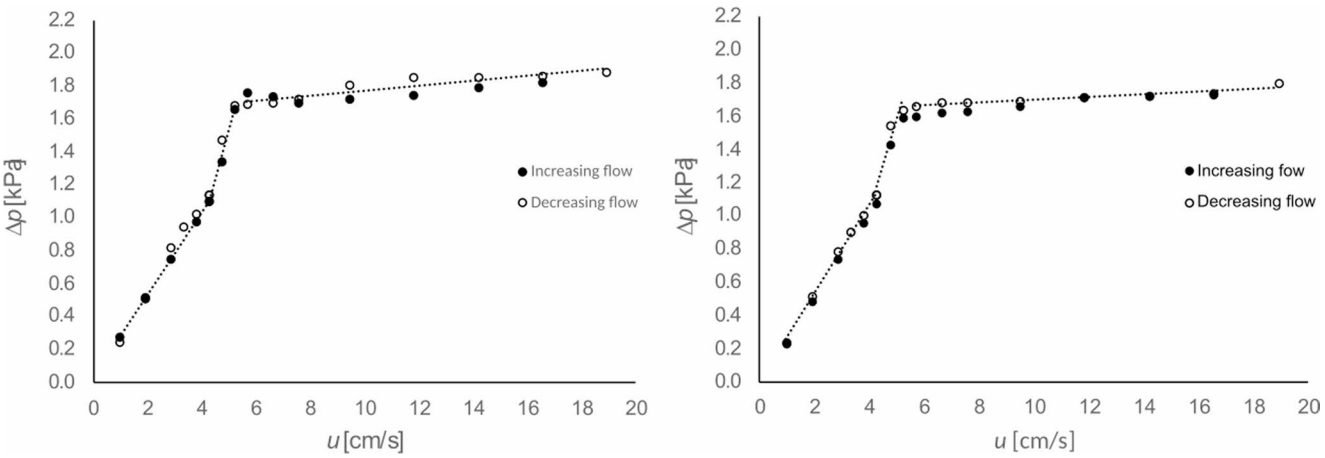

Fig. 6 Fluidization curves for sewage sludge of particle diameter between 300 µm – 500 µm (left) and its corresponding chars generated at 450 °C (right)

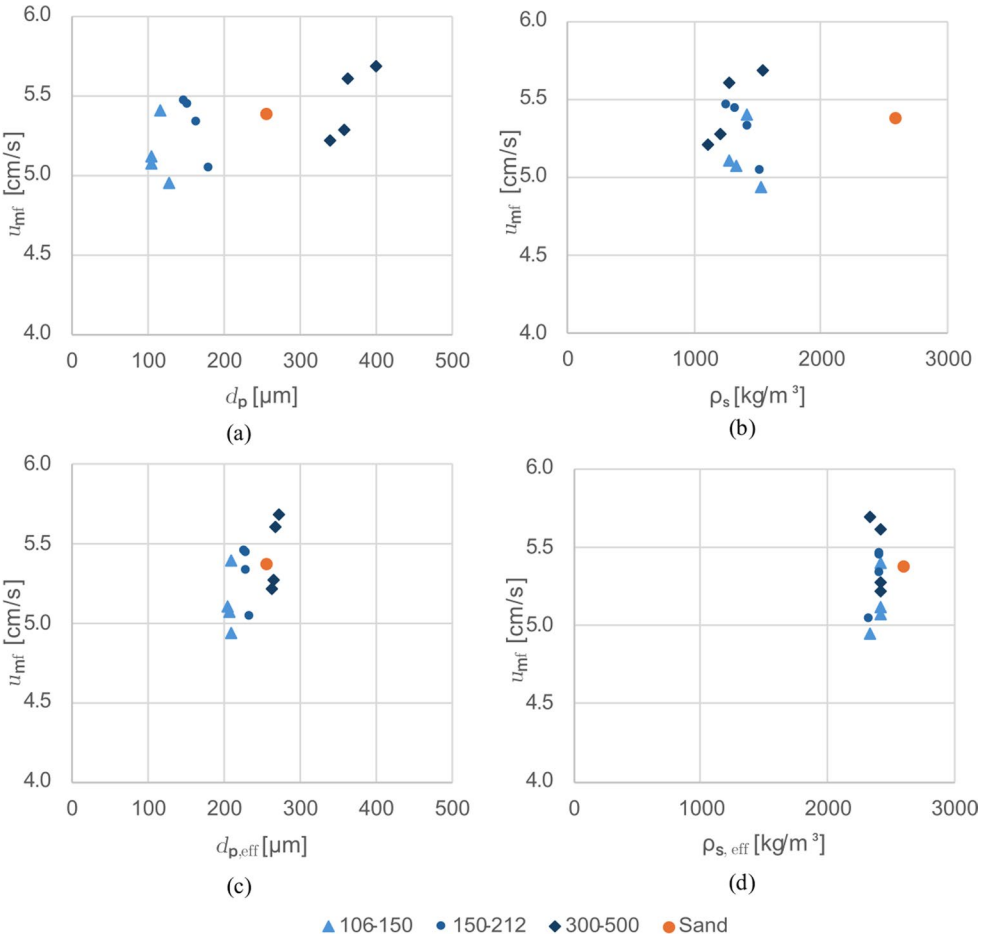

Fig. 7 Experimental values of u_{mf} of sewage sludge – sand and sewage sludge biochar – sand mixtures (**a**) compared to particle mean diameter of the sewage sludge and biochar, (**b**) compared to particle density of the sewage sludge and biochar, (**c**) compared to the effective particle mean diameter of the mixture with sand and (**d**) compared to the effective particle density of the mixture with sand

3.4 Prediction of minimum fluidization velocity sewage sludge – sand and sewage sludge biochar – sand mixtures

The minimum fluidization velocity of the binary mixtures can be predicted using Eq. 1 to determine $Re_{mf,\,eff}$, and subsequently u_{mf} using Eq. 2. First, a suitable pair of empirical factors, C_1 and C_2 from those in Table 1, to be used in Eq. 1 are selected. Then, a comparison is presented between the predicted (using the theoretical Ergun and the selected empirical factors) and the experimental values of u_{mf}. Figure 8 shows the relationship between Ar_{eff} and $Re_{mf,\,eff}$ (in continuous lines) obtained using the empirical correlation factors in Table 1 proposed by different authors and the experimental values for the binary mixtures determined in this study. The latter were calculated using the minimum fluidization velocity $u_{mf,}$ the effective particle mean diameter and the effective particle density obtained in the preceding sections together with the properties of air at ambient temperature and pressure in Eq. 2 and Eq. 3. The figure shows that, for each particle size range, there is a set of factors with which Eq. 1 best reproduce the experimental values of $Re_{mf,\,eff}$ for a given Ar_{eff}. For particles of the group 106 μm − 150 μm (S) experimental values are closer to the values calculated using the factors of Chitester et al. [29]. For particles of the group 150 μm – 212 μm (M) experimental values are closer to the ones obtained from Richardson et al. [25] or from Grace [28] as the factors of both authors are similar. Finally, for particles of the group 300 μm − 500 μm (L) experimental values correlate best to the values obtained using the factors proposed by Wen and Yu [24] .

Tables 4, 5 and 6 of the supplementary material include predicted values of u_{mf} according to each author presented in Table 1 and the corresponding relative error. Figure 9 show experimental and predicted u_{mf} values using the best set of factors for each particle size range and the ones calculated according to the Ergun equation. The best set of factors for each particle size range are determined from Fig. 8 and the minimum root mean square ratio (RMSE) presented in Table 7 of the supplementary material. The expressions used for the calculation of both relative error and RMSE are also included in the supplementary material.

For the medium particle size range RMSE calculated using Grace et al. [] is slightly lower than the one determined using

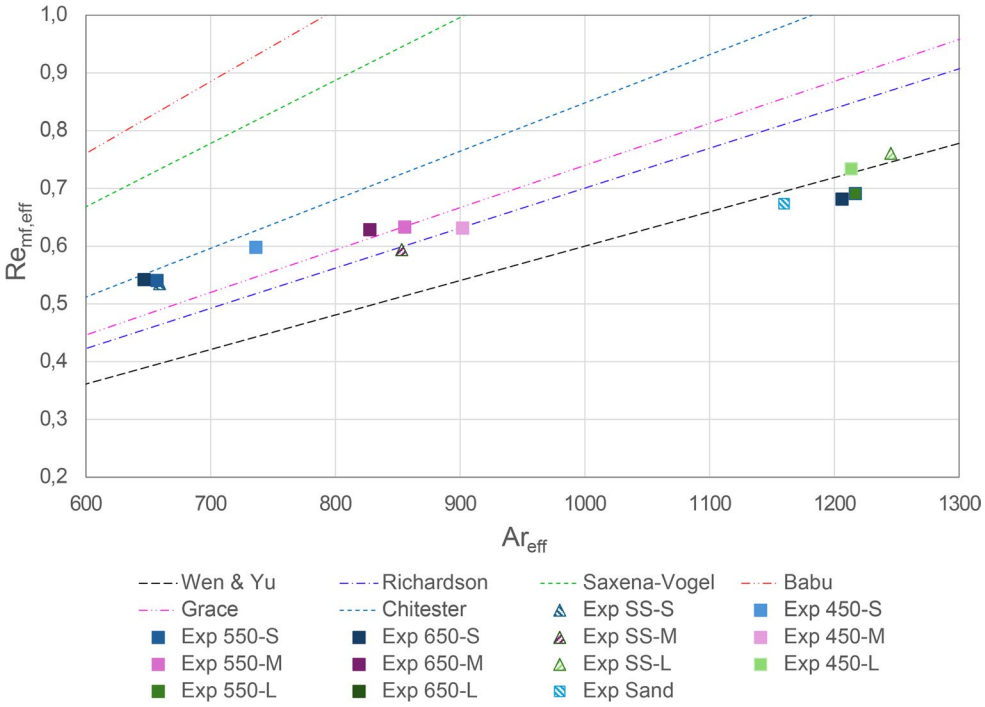

Fig. 8 Comparison between experimental and predicted values of $Re_{mf,\,eff}$. Predicted values are obtained by using Eq. 1 and the correlation factors C_1 and C_2proposed by different authors according to Table 1. Exp = Experimental value, S = 106 µm – 150 µm, M = 150 µm –212 µm, L = 300 µm – 500 µm

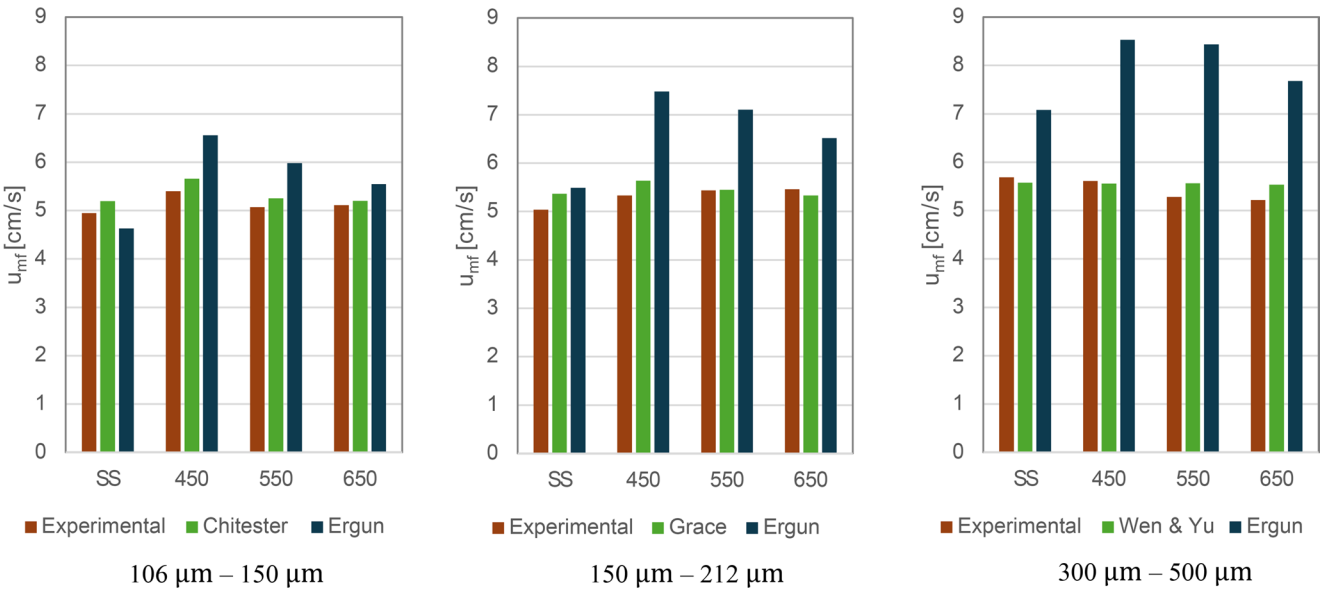

Fig. 9 Comparison of experimental and predicted values of u_{mf} of binary mixtures of sewage sludge – sand and sewage sludge biochar – sand. The predicted values are determined from $Re_{mf,\,eff}$ calculated using Eq. 1 with the best suited experimental factors for each particle size group and the factors according to the Ergun equation

the factors of Richardson et al. [25]. Relative errors for each sewage sludge and biochar particle size group are between 1.6% and 5.0% for the small mean particle diameter (106 µm − 150 µm) using the factors proposed by Chitester et al. [29]; between 0.2% and 6.5% for the group with the medium mean particle diameter (150 µm − 212 µm) using the factors proposed by Grace et al. [28] and between 1.0% and 6.0% using the factor proposed by Wen and Yu [24] for the group with the large mean particle diameter (300 µm − 500 µm). In all cases the values obtained using the factors based on the theoretical definition of the Ergun equation were found to be inaccurate in predicting u_{mf}. Uncertainty in the determination of the voidage and sphericity of the binary mixture affect the values of C_1 and C_2 and consequently u_{mf}.

3.5 Graphical determination of the fluidization regime during processing

Figure 10 shows the Grace diagrams where the sewage sludge and its biochars using different temperatures and fluidization velocities are presented. This diagram is used to determine the operating regime of a gas–solid fluidized bed [10]. The continuous lines and the area enclosed between them correspond to operation at the minimum fluidization velocity, while the green region represents the bubbling fluidized bed regime. The dashed line indicates the terminal velocity of the particles. Since particle properties change during the pyrolysis process, it is essential to assess whether the fluidization regime remains at minimum fluidization or transitions into the bubbling fluidization regime. The Grace diagram provides a framework to identify the fluidization regime of the bed before, during, and after pyrolysis. If the value of u^*increases above unity, the bed approaches operating conditions associated with the fast fluidization, turbulent fluidization and pneumatic transport regimes, which are not suitable for carrying out the process. The complete Grace diagram is presented in [10].

During biochar production in a fluidized bed reactor the fluidization velocity remains constant despite changes in particle properties. To determine how the change in particle properties during processing influence the fluidization regime, current analysis uses a constat fluidization velocity for each particle size, corresponding to the one determined for the sewage sludge particles. Crosses represent the location of the particles using u_{mf} at ambient temperature (20 °C) and empty circles the locations at the corresponding pyrolysis temperature of each sample. In all cases the higher the reaction temperature, the smaller the values of $u^*$and d^*. However, during processing, the binary mixture remains in the zone of minimum fluidization for all particle sizes. Figure 10 also shows how an increment in the velocity to 3 u_{mf} (filled circles) causes the particles to move closer to the bubbling fluidization regime. Since this regime is also optimal for fluidization it can be established that working with a gas velocity of 3 u_{mf} does not affect the operation. To reach turbulent or fast fluidization regimes further increases in the fluidization velocities have to be made.

4 Conclusions

Based on the analysis of the results, the following conclusions can be drawn:

- Both particle density and mean diameter decrease linearly with biochar yield during pyrolysis. The particles of the group 300–500 exhibit a slightly greater reduction in mean diameter and density.
- The reduction in particle size and density during pyrolysis shifts the biochar particles left and downward on the Geldart diagram in a linear pattern, but not enough to move them into group C.
- Increasing the mean particle diameter and density of the feedstock slightly increases the value of u_{mf}
- For each particle size group there is a correlation presented by Kunii and Levenspiel [10] that predicts the values of u_{mf} accurately. The values of u_{mf} obtained using the Ergun equation exhibited significant discrepancies, primarily due to inaccuracies in the determination of voidage and sphericity.

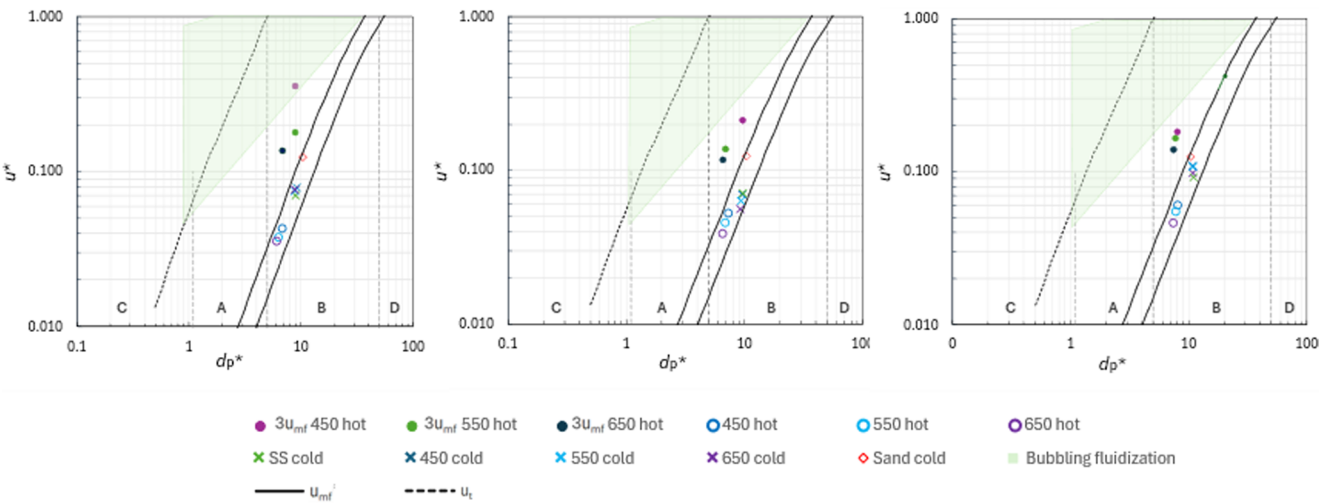

(a) 106 µm – 150 µm **(b)** 150 µm - 212 µm **(c)** 300 µm – 500 µm

Fig. 10 Grace diagrams for sewage sludge and its biochars

- According to the Grace diagram the pyrolysis temperature does not move the particles out of the minimum fluidization regime and working with a fluidization velocity of 3 u_{mf} moves the particles closer to the bubbling fluidization regime which means that the fluidization is not affected by the increase in gas velocity.
- During sewage sludge pyrolysis (using the sewage sludge of this study) in a fluidized bed reactor, the quality of fluidization is not adversely affected by changes in particle density or mean diameter. Consequently, no operational adjustments to process parameters are required during the reaction.

The findings of this study are applicable only to particles with chemical and physical properties comparable to those of the sewage sludge used herein. For particles with different characteristics which for example have a greater reduction in particle size and density a separate investigation following a similar methodology has to be made in order to accurately characterize the fluid dynamic behavior.

Supplementary Information The online version contains supplementary material available at https://doi.org/10.1007/s13399-026-07118-6.

Acknowledgements The authors sincerely appreciate the financial support provided by the Universidad Nacional de Colombia through the programs "Convocatoria nacional para el fortalecimiento de la formación a través del apoyo a proyectos de investigación, creación artística e innovación de la Universidad Nacional de Colombia 2022–2024 – Project code Hermes 57689", "Ingenio que transforma - Facultad de Ingeniería 2022 - Project code Hermes 58584" and the Sistema General de Regalias through the project "Desarrollo de una estrategia de valorización termoquímica de biosólidos a productos y bioenergía para el fortalecimiento de la economía circular y la sostenibilidad de la región Bogotá - BPIN 2020000100469".

Authors Contribution Andrés Felipe Pardo Martínez: Formal analysis, investigation, writing, review, editing, original draft, visualization. David Felipe Torres Arce: Formal analysis, investigation, writing, editing, original draft, visualization. Jorge Esteban Valbuena Mejía: Formal analysis, investigation, writing, original draft, visualization. Diana Carolina Guío-Pérez: Conceptualization, methodology, formal analysis, writing, review and editing, visualization, supervision. Sonia Lucía Rincón Prat: Conceptualization, methodology, formal analysis, writing, review and editing, visualization, supervision, project administration.

Funding Open Access funding provided by Colombia Consortium. The research leading to these results received funding from the Universidad Nacional de Colombia through the programs "Convocatoria nacional para el fortalecimiento de la formación a través del apoyo a proyectos de investigación, creación artística e innovación de la Universidad Nacional de Colombia 2022–2024 – Project code Hermes 57689", "Ingenio que transforma - Facultad de Ingeniería 2022 - Project code Hermes 58584" and the Sistema General de Regalias through the project "Desarrollo de una estrategia de valorización termoquímica de biosólidos a productos y bioenergía para el fortalecimiento de la economía circular y la sostenibilidad de la región Bogotá - BPIN 2020000100469".

Data availability Data available on request.

Declarations

Competing interests The authors declare that they have no known competing financial interests or personal relationships that could have appeared to influence the work reported in this paper.

References

1. World Bank Group Population growth (annual %), 2024. [Online]. Available: https://data.worldbank.org/indicator/SP.POP.GROW?name_desc. [Accessed abril 2024]
2. CAR PTAR El Salitre, 2024. [Online]. Available: https://www.car.gov.co/rio_bogota/vercontenido/9. [Accessed abril 2024]
3. Alférez Rivas LE, Nieves Pimiento N (2019) Plantas de tratamiento de aguas residuales (PTAR): impacto ambiental esperado e impacto ambiental provocado. Revista Caribeña de Ciencias Sociales (RCCS), pp. 6,42
4. Empresa De Acueducto y Alcantarillado de Bogotá E.S.P (2024)
5. Soria-Verdugo A, Morato-Godino A, Garcia-Gutierrez LM, Garcia-Hernando N (2017) „Pyrolysis of sewage sludge in a fixed and a bubbling fluidized bed – Estimation and experimental validation of the pyrolysis time. Energy Conv Manag 144:235–242
6. Schnell M, Horst T y, Quicker P (2020) «Thermal treatment of sewage sludge in Germany: A review,» *Journal of Environmental Management*, vol. 263, nº 110367
7. Varjúová D, Staňová AV, Grabicová K, Zakhar R, Bodík I (2023) Thermal methods of sludge processing—are they suitable for pharmaceuticals and illicit drugs removal from sewage sludge? Biomass Convers Biorefinery
8. Mendoza-Geney L, Rincón Prat S, Gómez A (2021) A comprehensive study of the high temperature pyrolysis of sewage sludge: kinetics, energy analysis and products formation. Glob NEST J 24:16–28
9. Fonts I, Gea G, Azuara M, Ábrego J, Arauzo J (2012) Sewage sludge pyrolysis for liquid production: a review. Renew Sustain Energy Rev 16:2781–2805
10. a. D (1991) L. O. Kunii, Fluidization engineering. Butterworth-Heinemann
11. Zhong W, Baosheng J, Zhang Y, Xiofang W (2008) Rui, „Fluidization of Biomass Particles in a Gas-Solid Fluidized Bed, *Energy and Fuels*. 22:4170–4176
12. Rao TR y, Bheemarasetti JR (2001) «Minimum fluidization velocities of mixtures of biomass and sands,» *Energy*, vol. 26, pp. 633–644
13. Clarke K, Pugsley T (2005) „Fluidization of moist sawdust in binary particle systems in a gas–solid fluidized bed. Chem Eng Sci 60:6909–6918
14. Berruti F, Liden A, Scott D (1988) „Measuring and modelling residence time distribution of low density solids in a fluidized bed reactor of sand particles. Chem Eng Sci 43(4):739–748

15. Kraft S, Kuba M, Hofbauer H (2018) The behavior of biomass and char particles in a dual fluidized bed gasification system. Powder Technol. https://doi.org/10.1016/j.powtec.2018.07.059
16. Paudel B, Feng Z-G (2013) Prediction of minimum fluidization velocity for binary mixtures of biomass and inert particles. Powder Technol 237:134–140
17. Oliveira T, Cardozo C, Ataíde C (2013) Bubbling fluidization of biomass and sand binary mixtures: minimum fluidization velocity and particle segregation. Chemical Engineering and Processing: Process Intensification. https://doi.org/10.1016/j.cep.2013.06.010
18. Khater E-S, Bahnasawy A, Hamouda R, Sabahy A, Abbas W, Morsy OM (2024) Biochar production under different pyrolysis temperatures with different types of agricultural wastes. Sci Rep 14(1):2625
19. Geldart D (1973) Types of gas fluidization. Powder Technol. https://doi.org/10.1016/0032-5910(73)80037-3
20. Grace J (1986) Contacting modes and behaviour classification of gas-solid and other two-phase suspensions. Can J Chem Eng. https://doi.org/10.1002/cjce.5450640301
21. Buczek B, Geldart D (1986) „Determination of the density of porous particles using very fine dense powders. Powder Technol 45:173–176
22. Cáceres-Martínez LE, Guío-Pérez DC, Rincón-Prat SL (2023) Significance of the particle physical properties and the Geldart group in the use of correlations for the prediction of minimum fluidization velocity of biomass–sand binary mixtures. Biomass Convers Biorefinery, pp. 1–17
23. Luckos A, Bunt J (2011) Pressure-drop predictions in a fixed-bed coal gasifier. Fuel 90:917–921
24. Wen C, Yu Y (1966) A generalized method for predicting the minimum fluidization velocity. AIChE J. https://doi.org/10.1002/aic.690120343
25. Richardson J, Harrison H, Davidson J (1971) Fluidization. Academic Press, New York
26. Saxena S, Vogel G (1977) The measurement of incipient fluidization velocities in a bed of coarse dolomite at temperature and pressure. Trans Institution Chem Eng, pp. 184–189
27. Babu S, Shah B, Talwalkar A (1978) Fluidization Correlations for Coal Gasification Materials - Minimum Fluidization Velocity and Fluidization Bed Expansion Ratio., *Alche*, pp. 176–186
28. Grace J (1982) Handbook of multiphase systems. Hemisphere, Washington D.C., pp 8–1
29. Chitester D, Kornosky R, Fan L, Danko J (1984) Characteristics of fluidization at high pressure. Chem Eng Sci. https://doi.org/10.1016/0009-2509(84)80025-1
30. Gupta S, Agarwal V, Singh S, Seshadri V, Mills D, Singh J (2009) Prediction of minimum fluidization velocity for fine tailings materials. Powder Technol. https://doi.org/10.1016/j.powtec.2009.08.003
31. Chongdian S, Qingjie G (2008) Fluidization characteristics of binary mixtures of biomass and quartz sand in an acoustic fluidized bed. Ind Eng Chem Res 47(23):9773–9782
32. Plantard G, Goetz V, Py X (2010) „A direct method for porous particle density characterization applied to activated carbons. Adv Powder Technol 21:592–598